Channel Measurement and Analysis of Human Body Radar Cross Section in 26 GHz ISAC Systems

DUAN Hongyu[1,2], WANG Mengyang[2], DUO Hao[3], HE Danping[2], MA Yihua[4], LU Bin[5], ZHONG Zhangdui[2]

(1. State Key Laboratory of Advanced Rail Autonomous Operation, Beijing Jiaotong University, Beijing 100044, China;
2. School of Electronic and Information Engineering, Beijing Jiaotong University, Beijing 100044, China;
3. CTTL Terminal Labs, China Academy of Information and Communication Technology, Beijing 100191, China;
4. State Key Laboratory of Mobile Network and Mobile Multimedia Technology, ZTE Corporation, Shenzhen 518055, China;
5. China Telecom Research Institute, Guangzhou 510630, China)

DOI: 10.12142/ZTECOM.202502002

https://kns.cnki.net/kcms/detail/34.1294.TN.20250517.1809.002.html, published online May 18, 2025

Manuscript received: 2024-12-13

Abstract: Radar cross section (RCS) plays a critical role in modeling target scattering characteristics and enhancing the precision of target detection and localization in integrated sensing and communication (ISAC) systems. This paper investigates the human body RCS at 26 GHz via multi-angle channel measurements under different clothing conditions. Based on calibrated electromagnetic (EM) parameters, the RCS characteristics of the human body in far-field conditions are analyzed using ray-tracing (RT) simulations. Some suggestions for the design of ISAC systems are also discussed. The results provide a solid theoretical foundation and practical reference for the modeling of target scattering characteristics for ISAC channels.

Keywords: channel measurement; human body; radar cross section; integrated sensing and communication; ray-tracing

Citation (Format 1): DUAN H Y, WANG M Y, DUO H, et al. Channel measurement and analysis of human body radar cross section in 26 GHz ISAC systems [J]. ZTE Communications, 2025, 23(2): 3 – 10. DOI: 10.12142/ZTECOM.202502002
Citation (Format 2): H. Y. Duan, M. Y. Wang, H. Duo, et al., "Channel measurement and analysis of human body radar cross section in 26 GHz ISAC systems," *ZTE Communications*, vol. 23, no. 2, pp. 3 – 10, Jun. 2025. doi: 10.12142/ZTECOM.202502002.

1 Introduction

6G technology drives the evolution of integrated sensing and communication (ISAC) systems. With its large bandwidth advantage, a 6G system allows perception functions to be upgraded from basic positioning to high-precision tracking, target recognition, and classification. Accurately perceiving key targets in ISAC channels is essential for achieving high-accuracy positioning and tracking[1].

In the research field of ISAC, the scattering characteristics of the human body as a typical target have attracted significant research attention. As a critical metric for evaluating the reflection characteristics of targets, the radar cross section (RCS) provides a critical reference basis for ISAC systems. With the rapid development of autonomous driving, healthcare, security monitoring, and other fields, the demand for high-precision object detection and recognition technology has surged[2–3]. In healthcare, the detected data can facilitate remote monitoring of vital signs and early detection of health issues, leveraging the advanced communication-sensing capabilities of 6G networks[4]. Furthermore, in search and rescue operations for survivors buried under avalanches, landslides, or collapsed buildings, RCS analysis of the human body can be promptly conducted to assess the situation and locate the trapped individuals. This capability enables precise localization and monitoring, facilitating efficient rescue operations and optimal resource allocation[2]. Other significant applications lie in the field of security, where this technology enables the identification and distinction of potentially dangerous individuals based on anomalous breath patterns or heartbeat patterns[5]. Human body RCS analysis further expands new applications for advanced technologies, such as multiple-input multiple-output (MIMO)[6], reconfigurable intelligent surface (RIS)[7–8], and micro-Doppler signature[9]. While there are ample application prospects and advantages, human body RCS analysis faces significant challenges. The radar simu-

This work was supported by the National Natural Science Foundation of China under Grant No. 62271043, Ministry of Education of China under Grant No. 8091B032123, and Beijing Natural Science Foundation under Grant No. L212029.

lation technique for human motion must be as close to the real radar data as possible; however, it must be easily implementable and computationally efficient at the same time[3].

Currently, most existing human detection radar systems operate in X-band, ultra-high frequency (UHF), and even lower frequency bands[10]. Ref. [11] discusses the findings of an RCS and specific absorption rate (SAR) study of the human head at 0.9 – 2.45 GHz based on full-wave numerical model simulations. The effective RCS of human cardiopulmonary activity is studied for a male subject in supine and prone positions at 2.4 GHz[12]. An experimental setup for complex channel measurement in a non-anechoic environment in the 6 – 10 GHz frequency range is validated in Ref. [13]. With the advancement of wireless communication towards higher frequency bands, such as millimeter-wave (mmWave), terahertz (THz), and visible light bands, an increasing overlap with traditional sensing frequency bands will occur[14]. Specifically, mmWave frequency bands are essential for 6G communication-sensing integration due to their remarkable capabilities, encompassing fine spatial resolution that enables high-precision target localization, speed measurement, and imaging[15]. Among mmWave frequencies, the 26 GHz band is particularly advantageous. It offers an effective balance between propagation characteristics suitable for long-range communications and the wide bandwidth essential for high-resolution sensing. Furthermore, the short wavelength of 26 GHz signals helps reduce interference from other cellular data, thereby enhancing spectrum efficiency.

Despite the recent execution of numerous ISAC channel measurements with human targets, a notable lack of data supporting human body RCS characteristics within the mmWave frequency bands poses a significant challenge for ISAC. Building on the limited existing literature, Ref. [16] presents detailed evaluations of human RCS characteristics. As an extension to prior analyses, it addresses open issues including the influence of different limb postures and clothing types on the 23 – 28 GHz frequency bands. However, precise data regarding the human body within the ISAC frequency band remains severely lacking, and various influential factors have not been comprehensively considered. Firstly, owing to its non-rigid nature, the human body undergoes numerous dynamic motions, leading to significant variations in the RCS depending on individual posture and radar orientation. Secondly, the human body is composed of multiple dielectric layers, which further complicates the RCS analysis. The roughness of skin and clothing surfaces introduces substantial variability in these analyses[17]. Additionally, existing studies often fail to provide direct electromagnetic (EM) material parameters for the human body during the RCS data analysis, thereby limiting the generalizability of research findings to other deterministic studies. Achieving far-field conditions for antenna and target channel measurements poses significant physical challenges. Ray-tracing (RT) techniques can effectively overcome these limitations, enabling precise calculation of RCS. However, current research still lacks RCS modeling in the multi-polarization mode under far-field conditions[18].

To address the above-mentioned demands and challenges, this paper conducts measurements and analyses of the human body within communication channels to provide a reference for implementing sensing functions through the communication systems. The main contributions and novelties of this paper are as follows.

• Channel measurements of the human body at 26 GHz are conducted on individuals wearing different clothing, capturing data from different angles in static situations. Based on these measurements, a comprehensive dataset of the human body is established.

• The EM material parameters related to the human body are calibrated. These parameters can be utilized for generalization simulations, providing a reference for deterministic modeling endeavors.

• The RCS at different azimuth and elevation angles is calculated and analyzed for different multi-polarization combinations. Based on these findings, suggestions for the future design of the ISAC system are discussed.

The rest of this paper is organized as follows. Section 2 describes the measurement system and campaign. Section 3 introduces the RT simulation and calibration of EM parameters. Section 4 presents a detailed RCS calculation and analysis, and Section 5 concludes the paper.

2 Measurement

2.1 Measurement System

In this work, the measurement system comprises a Keysight N5247A vector network analyzer (VNA), a personal computer (PC) control terminal, and two standard gain horn antennas, as depicted in Fig. 1. The VNA, connected to the PC and controlled by specialized programs, generates signals with a bandwidth of 1 GHz and acquires 201 frequency samples. The an-

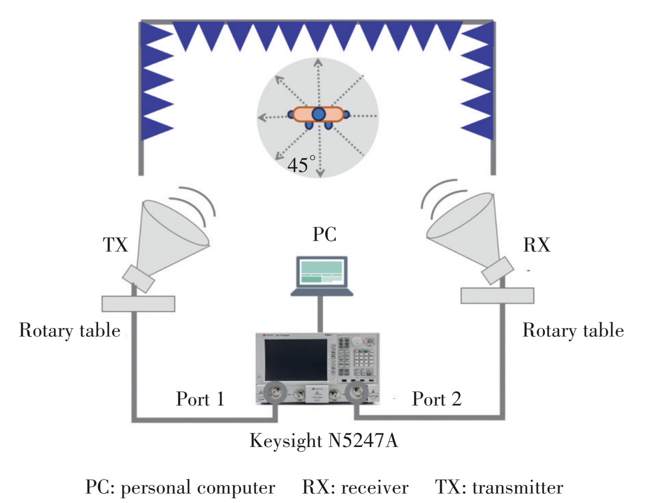

Figure 1. Measurement system

tennas, serving as the transmitter (TX) and receiver (RX), are fixed on separate rotary tables and connected to Port 1 and Port 2 of the VNA, respectively. The system is set up in a semi-dark room with the antennas positioned at ±34° angles toward the human body, maintained at a distance of 1.6 m and a height of 1.01 m above the ground. This configuration ensures that the main lobe of the TX illuminates the human body, while the RX receives the corresponding echo. The configuration parameters of the measurement system are summarized in Table 1.

2.2 Measurement Campaign

The channel measurement of the human body at multiple angles is carried out in a semi-dark room built with absorbing materials. The subject is an adult male (1.78 m in height, 78 kg in weight) wearing two kinds of clothing (short and long clothes), as shown in Fig. 2. The point cloud of the subject's body is obtained by laser scanning. After processing the point cloud and importing it into SketchUp to give the corresponding materials to the human body surface, the human body model used in RT simulation is established.

To obtain the scattering characteristics of the human body at different angles, five rotational positions of the human body relative to the measurement system are set up. The subject stands on a rotary table to control the rotation angle by the scale. The 0° position corresponds to the human body directly facing the measurement system, and the other four positions are set at 45°, 90°, 135°, and 180° in the clockwise direction. The measurement results under different clothing conditions are shown in Figs. 3 and 4. The absorbing material effectively shields the echoes from many environmental objects, and the multipath component (MPC) of the human body is marked.

The results show that the power of MPC of the human body is the strongest when facing the measurement system and facing away from it, which are rotating at 0° and 180°. In these two cases, the reflection and scattering area of the human body is larger, so the reflected echo energy is larger. The human back approximates a convex surface, resulting in the strongest reflection power. This is because the convex surface concentrates the reflected waves into a smaller area, thereby increasing the power density of the reflected signal in the direction of reflection. Meanwhile, the power of MPC under short clothes is higher than that under long clothes, which can be explained by the fact that human skin is smoother than clothing, and its echo power of reflection and scattering is stronger. However, in the case of rotating at 180°, the back in long clothes is flatter than that in short clothes, so the reflected power is stronger than that under short clothes. Additionally, the body posture observed in this study often has the limbs close to the body, making it challenging to accurately identify different body parts using only the power delay profile (PDP).

Table 1. Configuration parameters of the measurement system

Measurement Parameter	Value
Center frequency	26 GHz
Bandwidth	1 GHz
Delay resolution	1 ns
Frequency samples	201
TX and RX heights from the ground	1.01 m
Distance between TX and RX	1.6 m
Antenna rotation angle towards the human body	±34°
Polarization mode	Vertical polarization
Antenna gain	22.4 dBi

RX: receiver TX: transmitter

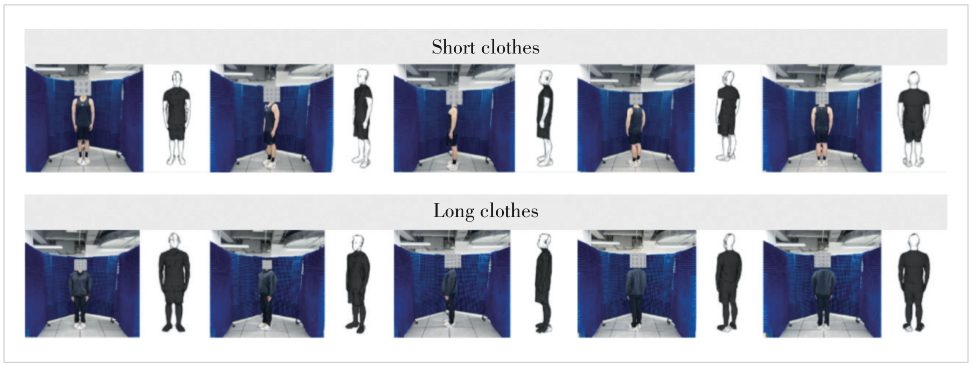

Figure 2. Human body in different types of clothes

3 RT Simulation and Calibration of EM Parameters

3.1 RT Simulation

In this work, the high-performance RT simulation platform developed by the State Key Laboratory of Advanced Rail Autonomous Operation of Beijing Jiaotong University is adopted[19–20]. In ISAC channels, the scattering characteristics of targets are crucial for accurate channel modeling, which is affected by the dominant propagation mechanisms of reflection and scattering. Fresnel reflection and directional scattering[21] are applied in RT.

3.1.1 Reflection

When an object whose volume is much larger than the wavelength of the EM wave is in the path of propagation, the wave cannot diffract through the object and will be reflected at the junction of different media. The wireless signal reflected by the ground or other obstacles reaches the receiver, called the reflected wave. The electric field strength of the reflected wave and transmitted wave depends on the Fresnel reflection coefficient of the incident wave in the medium. The coefficients $r_{\parallel i,k}$ and $r_{\perp i,k}$ are

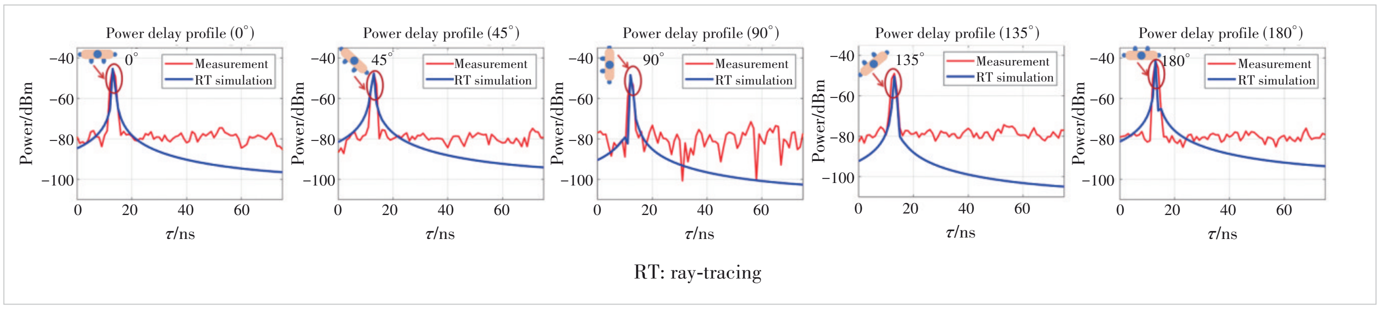

Figure 3. Measurement results of the subject in short clothes

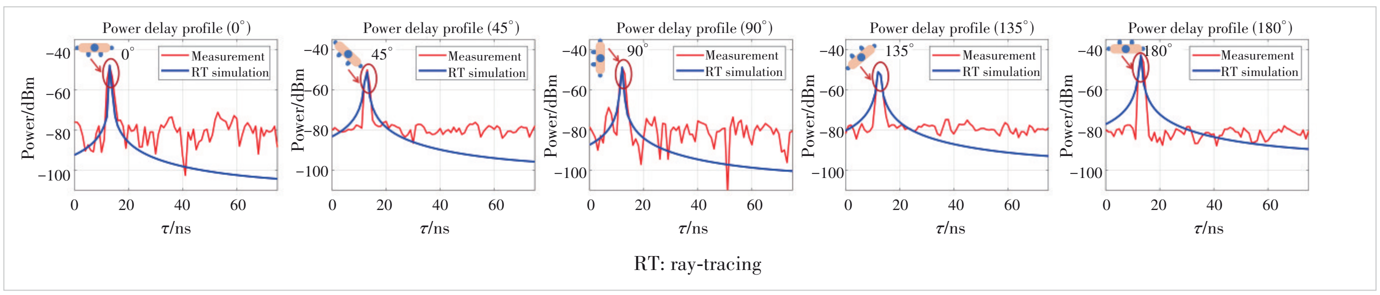

Figure 4. Measurement results of the subject in long clothes

the reflection (scattering) coefficients of the vertical and horizontal components of the k-th multipath component at the i-th reflection (scattering) surface, respectively. For transversal magnetic (TM) polarization, the reflection coefficient is:

$$r_{\parallel i,k} = R_{\mathrm{TM}_{i,k}} = \frac{\sqrt{\frac{\varepsilon_2}{\varepsilon_1}}\cos\delta_{\mathrm{inc}_{i,k}} - \cos\delta_{\mathrm{trans}_{i,k}}}{\sqrt{\frac{\varepsilon_2}{\varepsilon_1}}\cos\delta_{\mathrm{inc}_{i,k}} + \cos\delta_{\mathrm{trans}_{i,k}}} \quad (1).$$

For transversal electric (TE) polarization, the reflection coefficient is:

$$r_{\perp i,k} = R_{\mathrm{TE}_{i,k}} = \frac{\cos\delta_{\mathrm{inc}_{i,k}} - \sqrt{\frac{\varepsilon_2}{\varepsilon_1}}\cos\delta_{\mathrm{trans}_{i,k}}}{\cos\delta_{\mathrm{inc}_{i,k}} + \sqrt{\frac{\varepsilon_2}{\varepsilon_1}}\cos\delta_{\mathrm{trans}_{i,k}}} \quad (2).$$

For the TM case, the magnetic field component is parallel to the reflection (scattering) surface. However, for the TE case, the electric field component is parallel to the reflection (scattering) surface. The angles $\delta_{\mathrm{inc}_{i,k}}$ and $\delta_{\mathrm{trans}_{i,k}}$ are the incidence and transmission angles, respectively, with respect to the normal vector of the surface where reflection (scattering) occurs.

3.1.2 Scattering

There are two kinds of scattering models in wireless communication: the directional scattering and RCS scattering. The former includes the directional single-beam model and the directional double-beam model. The directional single-beam model is mainly introduced here. This model assumes that the scattered lobes reflect in the direction of the mirror surface, and the expression is as follows:

$$\left|E_S\right|^2 = \left|E_{S_0}\right|^2\left(\frac{1+\cos\psi}{2}\right)^{\alpha_R},\ \alpha_R = 1, 2, \cdots, N \quad (3),$$

where ψ denotes the angle formed between the scattering and reflection directions; α_R represents the scattering equivalent roughness, an integer that dictates the width of the scattering lobe, with increasing values resulting in narrower beams; E_S signifies the scattered electric field, measured at an angle ψ from the reflection direction; E_{S_0} signifies the maximum scattered electric field value. When the EM wave is incident on the surface of the material at the incident angle θ_i, E_{S_0} is expressed as follows:

$$\left|E_{S_0}\right|^2 = \left(\frac{SK}{d_t d_r}\right)^2 \frac{\mathrm{d}S\cos\theta_i}{F_{\alpha_R}} \quad (4).$$

Extending the unit area of the material surface dS (the length of the scatterer is l and the width is unit length), we get the final expression of the DS model as follows:

$$\left|E_S\right|^2 = \left|E_{S_0}\right|^2\left(\frac{1+\cos\Psi}{2}\right)^{\alpha_R} = \left(\frac{SK}{d_t d_r}\right)^2 \frac{l\cos\theta_i}{F_{\alpha_R}}\left(\frac{1+\cos\Psi}{2}\right)^{\alpha_R} \quad (5),$$

where l represents the length of the scatterer, K is a constant that depends on the incident power P_t and antenna gain G_t, $K =$

$\sqrt{60P_tG_t}$, and F_{α_R} is the proportionality factor.

3.2 Calibration of EM Parameters

EM parameters of materials are the foundation of RT, enabling effective representation of the interactions between targets and surroundings. Accurate EM parameters not only enhance the generalization capability of RT across different application scenarios but also improve its predictive accuracy in complex environments. Before calibration of EM parameters, the system and cable losses are measured to ensure accuracy.

Multiple key EM parameters of the human body are calibrated, including the real part of relative permittivity ϵ_{rel}, the loss tangent δ, the scattering gain S, and the effective smoothness α_R. The EM parameters can also describe the body's absorption of radio waves to a certain extent. As shown in Fig. 5, the EM parameters are calibrated based on the power of MPC. The EM parameters of the relevant materials are continuously updated until the error between the simulation power and the measurement power converges. The initialized and calibrated EM parameters are summarized in Table 2.

Table 3 shows the errors between the power of calibrated simulation and measurement, including cases at multiple rotating angles. The calibrated RT can accurately describe the scattering characteristics of the human body at multiple angles with a mean absolute error of 0.82 dB and a standard deviation of 0.89 dB.

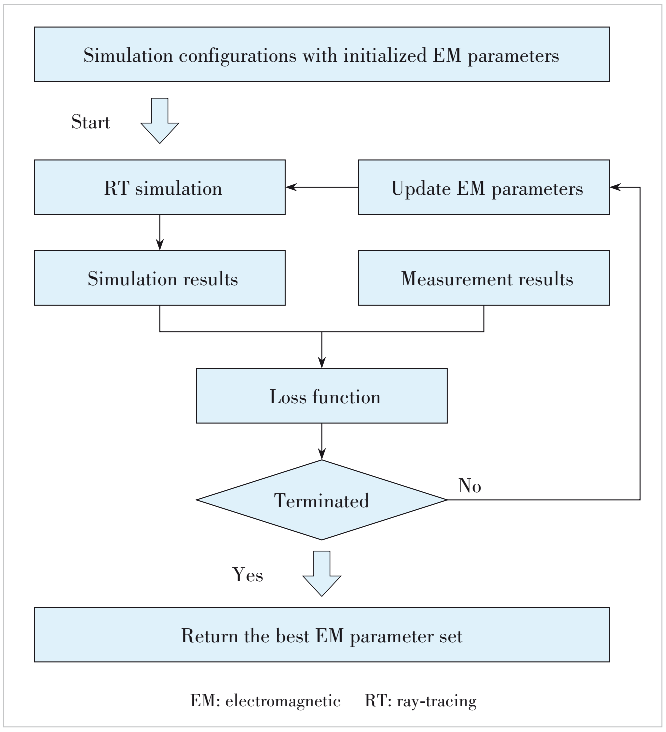

Figure 5. Working flow of calibration of EM parameters

Table 2. Comparison of initialized and calibrated EM parameters.

Material	Initialized				Calibrated			
	ϵ_{rel}	δ	S	α_R	ϵ_{rel}	δ	S	α_R
Skin	1	0.1	1	1	17.7	0.953 1	0.88	16.5
Polyester	1	0.1	1	1	2.1	0.750 0	0.85	15.3
Cotton	1	0.1	1	1	2.8	0.700 0	0.83	14.2

Table 3. Error statistics

Outfit	Angle/(°)	Measurement Power/dBm	Simulation Power/dBm	Absolute Error/dB
Short	0	−45.20	−45.34	0.14
	45	−47.37	−47.70	0.36
	90	−49.85	−48.40	1.45
	135	−49.01	−50.45	1.44
	180	−41.36	−41.52	0.16
Long	0	−48.05	−47.93	0.12
	45	−50.05	−51.30	1.25
	90	−48.71	−48.85	0.14
	135	−51.30	−51.11	0.19
	180	−39.51	−42.44	2.93

4 Analysis of RCS

4.1 Calculation of RCS

RCS plays a key role in target sensing and recognition in ISAC channels, as it directly impacts the reflection and scattering characteristics. The RCS σ can be calculated based on the receiving power P_r of the multipath, as shown in:

$$\sigma = \frac{P_r(4\pi)^3 R^4}{P_t G_t G_r \lambda^2} \tag{6}$$

where P_t is the transmitting power, λ is the wavelength, and R is the range between the target and the measurement system. The gains G_t and G_r represent the transmitting and receiving antenna gains.

Near-field effects arise near the radiating element, where the EM field is incomplete, causing significant inductive and capacitive coupling. Conversely, far-field effects, observed at distances where waves have propagated as plane waves, minimize coupling impacts. However, due to the physical limitations of the measurement systems and environments, it is often difficult to ensure that both the antenna and the target are in the far-field region[22]. When the target and the antenna are in the far field, the EM waves can be approximated as plane waves. This facilitates the calculation and prediction of scattering characteristics, ensuring the stability and consistency of measurement results. If not, near-field effects may significantly degrade measurement accuracy, leading to erroneous analysis outcomes. In such cases, RT, with its flexibility, breaks scenario constraints, making it an effective tool for calculating RCS.

The distance between the human body and RX is 1.80 m. The maximum size of the human body is 1.78 m. According to the equation:

$$d_f = 2D^2/\lambda \quad (7),$$

where d_f is the distance of the Fraunhofer region, D is the maximum linear dimension of the antenna, and λ is the wavelength. The far-field distance of the human body is 561.6 m. In the simulation of this work, the distance between the human body and the measurement system is set to 580 m to ensure that both the human body and antennas are in the far field.

In ISAC systems, the variation of RCS at different azimuth angles is essential for describing a target's scattering characteristics. Since RCS represents how a target reflects EM waves, its variation with angle directly influences sensing accuracy and communication channel performance. On the other hand, the research of RCS at different zenith angles is also very important for the deployment of ISAC systems. The TX-RX polarization combinations include horizontal-horizontal (H-H), horizontal-vertical (H-V), vertical-horizontal (V-H), and vertical-vertical (V-V) polarizations. As shown in Figs. 6 and 7, the RCSes of the human body at different horizontal and elevation angles under different clothing are calculated by RT. Table 4 shows the statistics of RCS under different polarization modes.

The findings reveal that the RCS is typically greater when the TX and RX antennas are aligned in the same polarization mode. Furthermore, the RCS for short clothing tends to be slightly higher than that for long clothing in the same polarization mode. Notably, the mean azimuth RCS, when subjected to different polarization modes, experiences a decrease of approximately 16 dBsm compared to that in the same polarization mode. The mean elevation RCS sees a reduction of around 14 dBsm under similar circumstances.

4.2 System Design Discussion

The calculation of RCS indicates that the RCS values are higher when using co-polarized transmit and receive antennas, which can be attributed to the EM scattering characteristics of co-polarization. In a co-polarization configuration, the polarization of the TX and RX antennas is aligned, allowing for more efficient capture of the reflected signals from the target. This alignment enables better matching between the incident wave and the target's scattering properties, particularly for surfaces with geometric regularity or dimensions comparable to the wavelength, resulting in stronger energy coupling and consequently higher RCS values. From an EM theory perspective, the target's

Table 4. Statistics of RCS under different polarization modes

Outfit	Polarization	Mean Azimuth RCS/dBsm	Polarization	Mean Elevation RCS/dBsm
Short	H-H	−2.78	H-H	−7.83
	H-V	−19.3	H-V	−22.21
	V-H	−19.3	V-H	−22.21
	V-V	−2.52	V-V	−7.45
Long	H-H	−3.91	H-H	−8.17
	H-V	−18.82	H-V	−21.91
	V-H	−18.82	V-H	−21.91
	V-V	−3.59	V-V	−7.54

H-H: horizontal-horizontal RCS: radar cross section V-V: vertical-vertical
H-V: horizontal-vertical V-H: vertical-horizontal

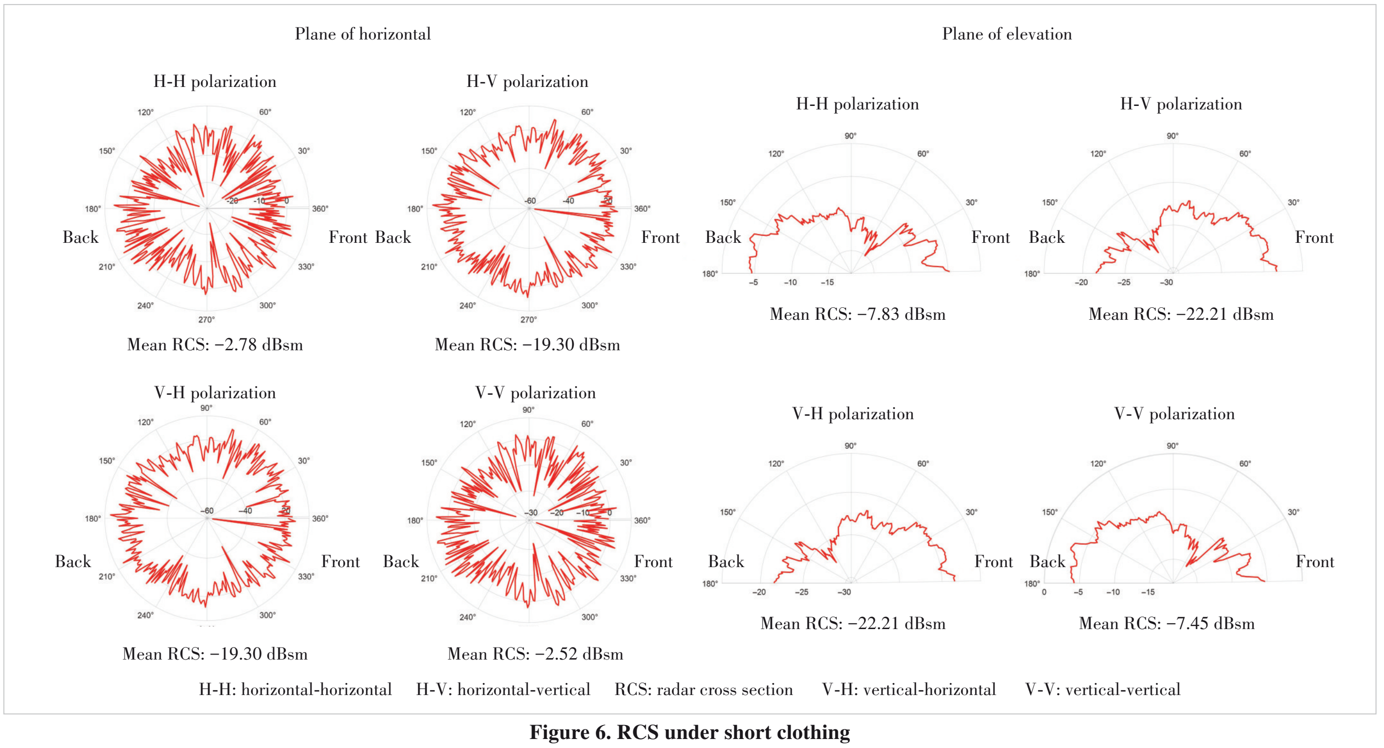

Figure 6. RCS under short clothing

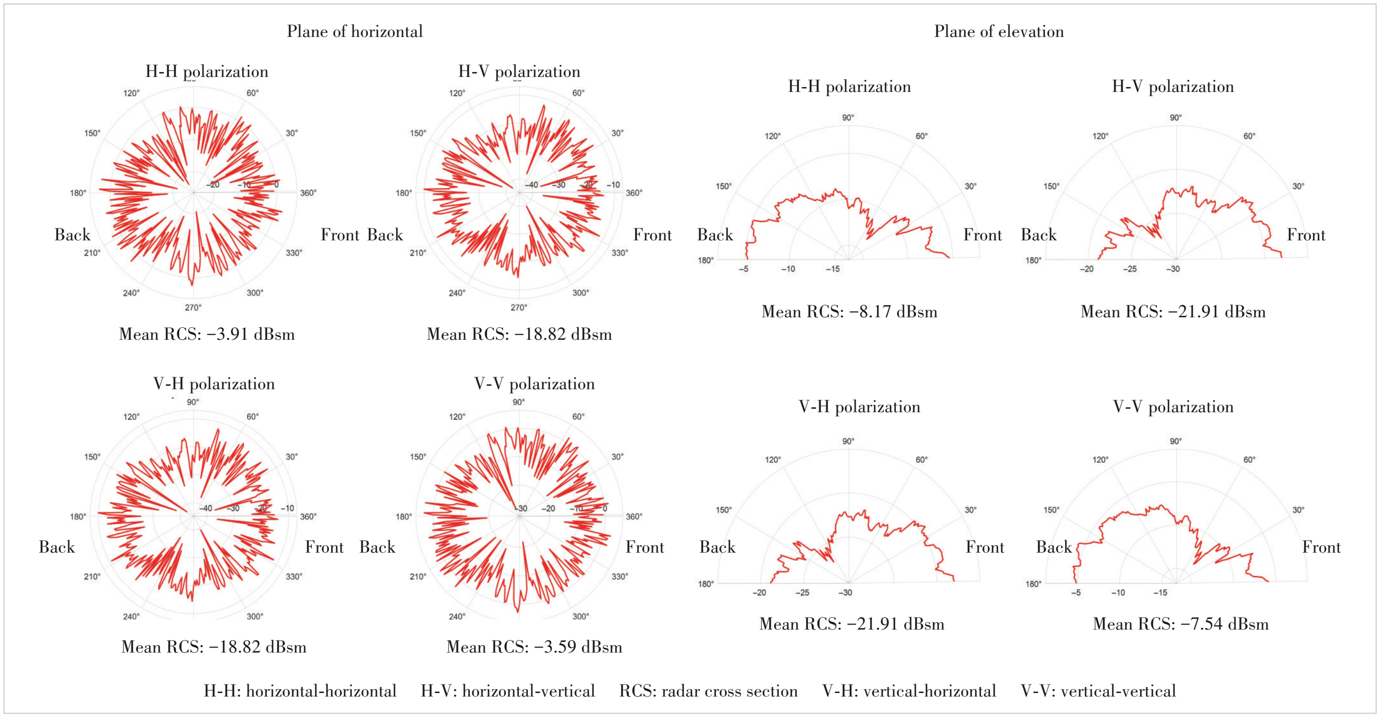

Figure 7. RCS under long clothing

surface induces scattering, reflection, and absorption of the EM waves. Under co-polarized conditions, the reflection coefficient is relatively high. For complex targets such as the human body, various factors, including the surface roughness, material composition, EM parameters, and clothing conditions, can significantly influence RCS. The co-polarization setup enhances the coherence of reflected signals, thereby increasing the strength of the scattered signals. Furthermore, as EM waves undergo multiple reflections on the target's surface, co-polarization tends to facilitate phase addition, further amplifying the magnitude of the received signal.

The research content of this paper aims to analyze the characteristics of the target in the communication channel to realize the sensing function. Therefore, in the design of this kind of ISAC systems, opting for co-polarized TX and RX configurations can effectively enhance the echo signal from the target, improving detection sensitivity. It also enhances the system's resilience to interference and reduces the impact of background noise, thereby improving sensing accuracy and robustness. Such a design is particularly suitable for scenarios requiring high sensitivity and precise sensing, such as long-range target detection and weak scattering characteristic capture.

However, interference may distort the reflected signal, leading to fluctuations or attenuation of the RCS. The movement of a target in a dynamic environment alters its reflective characteristics, causing the RCS to vary with the incident angle. Multipath effects may further exacerbate the impact. In the future, we need to consider measuring in more element-rich scenarios to fully account for these influencing factors.

5 Conclusions

This paper presents multi-angle channel measurements of the human body at 26 GHz under different clothing conditions. Based on the measurement data, the EM parameters of human body materials are calibrated with a mean absolute error of 0.82 dB and a standard deviation of 0.89 dB. The RT simulator is deployed to comprehensively calculate and analyze the RCS of the human body under various polarization configurations, azimuth angles, and elevation angles. The results indicate that co-polarized antennas exhibit higher RCS values across a range of angles compared to cross-polarized configurations. Finally, some suggestions on the design of ISAC systems are given. This work not only highlights the significant impact of polarization on target scattering characteristics but also provides critical insights for target identification and environmental sensing. The data and results presented in this work offer theoretical support and practical guidance for the design of ISAC systems.

References

[1] INCA S, MROZOWSKI A, PRADO-ALVAREZ D, et al. Angular correlation study of sensing and communication channels in V2X scenarios for 6G ISAC usage [C]//Proc. IEEE Globecom Workshops (GC Wkshps). IEEE, 2023: 1189–1194. DOI: 10.1109/GCWkshps58843.2023.10465114
[2] DE PASQUALE G, SARRI A, BONOPERA C, et al. RCS of human being physiological movements in the 1–10 GHz bandwidth: theory, simulation and measurements [C]//Proc. IEEE Radar Conference. IEEE, 2008: 1–6. DOI: 10.1109/RADAR.2008.4720983
[3] ISHAK K, APPENRODT N, DICKMANN J, et al. Advanced radar micro-Doppler simulation environment for human motion applications [C]//Proc.

IEEE Radar Conference (RadarConf). IEEE, 2019: 1 – 6. DOI: 10.1109/RADAR.2019.8835755

[4] KIRIAZI J E, BORIC-LUBECKE O, LUBECKE V M. Radar cross section of human cardiopulmonary activity for recumbent subject [C]//Annual International Conference of the IEEE Engineering in Medicine and Biology Society. IEEE, 2009: 4808 – 4811. DOI: 10.1109/IEMBS.2009.5332634

[5] KIRIAZI J E, BORIC-LUBECKE O, LUBECKE V M. Modeling of human torso time-space characteristics for respiratory effective RCS measurements with Doppler radar [C]//Proc. IEEE MTT-S International Microwave Symposium. IEEE, 2011: 1. DOI: 10.1109/MWSYM.2011.5973284

[6] HONMA N, SASAKAWA D, SHIRAKI N, et al. A state-machine-based approach for human activity classification using MIMO radar [C]//Proceedings of International Symposium on Antennas and Propagation (ISAP). IEEE, 2021: 1 – 2. DOI: 10.23919/ISAP47258.2021.9614433

[7] SHEN Y, OU P, CHEN F K, et al. Reconfigurable intelligent surface-assisted channel characteristics in 5G high-speed railway scenario [J]. Journal of Beijing Jiaotong University, 2023, 47(2): 23 – 35. DOI: 10.11860/j.issn.1673-0291.20220098

[8] HAN F Y, DING J M, FEI D, et al. Channel parameter acquisition and simulation evaluation of RIS-aided wireless communication system [J]. Journal of Beijing Jiaotong University. 2023, 47(5): 63 – 71. DOI: 10.11860/j.issn.1673-0291.20220147

[9] ABADPOUR S, PAULI M, SCHYR C, et al. Angular resolved RCS and Doppler analysis of human body parts in motion [J]. IEEE transactions on microwave theory and techniques, 2023, 71(4): 1761 – 1771. DOI: 10.1109/TMTT.2022.3218304

[10] SINGH A D, RAM S S, VISHWAKARMA S. Simulation of the radar cross-section of dynamic human motions using virtual reality data and ray tracing [C]//Proc. IEEE Radar Conference (RadarConf18). IEEE, 2018: 1555 – 1560. DOI: 10.1109/RADAR.2018.8378798

[11] FANG C H, QIN Y, HU C-F. Numerical study of human head RCS and SAR at 0.9 – 2.45 GHz [C]//2017 International Applied Computational Electromagnetics Society Symposium (ACES). IEEE, 2017: 1 – 2

[12] LEE A, GAO X M, XU J, et al. Effects of respiration depth on human body radar cross section using 2.4 GHz continuous wave radar [C]//Proc. 39th Annual International Conference of the IEEE Engineering in Medicine and Biology Society (EMBC). IEEE, 2017: 4070 – 4073. DOI: 10.1109/EMBC.2017.8037750

[13] TIEN T V, OUVRY L, SIBILLE A. Time domain complex radar cross section of human body for breath-activity monitoring [C]//Proc. 11th European Conference on Antennas and Propagation (EUCAP). IEEE, 2017: 421 – 425. DOI: 10.23919/EuCAP.2017.7928648

[14] YANG B, LIANG X, LIU S N, et al. Intelligent 6G wireless network with multi-dimensional information perception [J]. ZTE communications, 2023, 21(2): 3 – 10. 10.12142/ZTECOM.202302002

[15] LIU H P, ZHANG X Y, ZHOU A F, et al. Indoor environment and human sensing via millimeter wave radio: a review [J]. ZTE communications, 2021, 19(3): 22 – 29. DOI: 10.12142/ZTECOM.202103004

[16] SCHUBERT E, KUNERT M, MENZEL W, et al. Human RCS measurements and dummy requirements for the assessment of radar based active pedestrian safety systems [C]//14th International Radar Symposium (IRS). IEEE, 2013: 752 – 757

[17] ABADPOUR S, MARAHRENS S, PAULI M, et al. Backscattering behavior of vulnerable road users based on high-resolution RCS measurements [J]. IEEE transactions on microwave theory and techniques, 2022, 70(3): 1582 – 1593. DOI: 10.1109/TMTT.2021.3131156

[18] MANFREDI G, RUSSO P, DE LEO A, et al. Efficient simulation tool to characterize the radar cross section of a pedestrian in near field [J]. Progress in electromagnetics research C, 2020, 100: 145 – 159. DOI: 10.2528/pierc19112701

[19] HE D P, AI B, GUAN K, et al. The design and applications of high-performance ray-tracing simulation platform for 5G and beyond wireless communications: a tutorial [J]. IEEE communications surveys & tutorials, 2019, 21(1): 10 – 27. DOI: 10.1109/COMST.2018.2865724

[20] HE D P, GUAN K, YAN D, et al. Physics and AI-based digital twin of multi-spectrum propagation characteristics for communication and sensing in 6G and beyond [J]. IEEE journal on selected areas in communications, 2023, 41(11): 3461 – 3473. DOI: 10.1109/JSAC.2023.3310108

[21] DEGLI-ESPOSTI V, FUSCHINI F, VITUCCI E M, et al. Measurement and modelling of scattering from buildings [J]. IEEE transactions on antennas and propagation, 2007, 55(1): 143 – 153. DOI: 10.1109/TAP.2006.888422

[22] HUANG J H, ZHOU J J, DENG Y. Near-to-far field RCS calculation using correction optimization technique [J]. Electronics, 2023, 12(12): 2711. DOI: 10.3390/electronics12122711

Biographies

DUAN Hongyu received his BE degree in information engineering from the School of Electronic and Information Engineering, Beijing Jiaotong University, China in 2022. He is currently pursuing a PhD degree at the State Key Laboratory of Advanced Rail Autonomous Operation, Beijing Jiaotong University. His research interests include radio wave propagation, wireless channel modeling, and integrated sensing and communication.

WANG Mengyang received his BE degree in communication engineering from University of Jinan, China in 2024. He is pursuing a master's degree at the School of Electronic and Information Engineering, Beijing Jiaotong University, China. His research interests include wireless channel modeling and integrated sensing and communication.

DUO Hao (duohao@caict.ac.cn) is the Deputy Chief Engineer of CTTL-terminal at the China Academy of Information and Communications Technology. He has been engaged in the research of wireless mobile communication technology for a long time. He has extensive experience in mobile terminal standardization work, both domestically and internationally, with a particular focus on mobile terminal device testing technology. He has completed over 30 industry-standard projects in China's mobile terminal industry and published over 10 papers in important domestic journals.

MA Yihua received his BE degree from Southeast University, China in 2015 and MS degree from Peking University, China in 2018. Since 2018, he has been with ZTE Corporation. He is now a senior expert in the Department of Wireless Algorithm of ZTE, and a member of the State Key Laboratory of Mobile Network and Mobile Multimedia Technology, China. His main research interests include integrated sensing and communications, distributed massive MIMO, and grant-free NOMA.

HE Danping is an associate professor with the School of Electronic and Information Engineering, Beijing Jiaotong University, China. Her current research interests include radio propagation and channel modeling, ray-tracing technologies, and wireless communication algorithm design. She received five best paper awards and the 2019 Applied Computational Electromagnetics Society (ACES)-China Young Scientist Award.

LU Bin received his master's and PhD degrees from the Department of Radio Engineering, South China University of Technology, China. He is now a senior engineer at the China Telecom Research Institute. His current research interests include wireless private networks, radio propagation and channel modeling, and wireless mobile digital twin technology.

ZHONG Zhangdui is a professor with the School of Electronic and Information Engineering, Beijing Jiaotong University, China. He is also a director of the Innovative Research Team of the Ministry of Education, China, and a Chief Scientist of the Ministry of Railways of China. He is an executive council member of the Radio Association of China and a deputy director of the Radio Association of Beijing, China. His research interests are wireless communications for railways, control theory and techniques for railways, and the GSM-R system.